

Available online at www.sciencedirect.com

ScienceDirect

journal homepage: <http://www.elsevier.com/locate/rpor>

Original research article

Monte Carlo calculation of photo-neutron dose produced by circular cones at 18 MV photon beams

Elham Hosseinzadeh^a, Nooshin Banaee^a, Hassan Ali Nedaie^{b,c,*}^a Department of Medical Radiation, Engineering Faculty, Central Tehran Branch, Islamic Azad University, Tehran, Iran^b Odette Cancer Centre, University of Toronto, Toronto, Canada^c Joint Cancer Research Center, Radiotherapy Oncology & Radiobiology Research Center, Cancer Institute, Tehran University of Medical Sciences, Tehran, Iran

ARTICLE INFO

Article history:

Received 13 May 2017

Received in revised form

14 August 2017

Accepted 11 December 2017

Available online 9 January 2018

Keywords:

Circular cones

Neutron equivalent dose

Neutron fluence

Monte Carlo

ABSTRACT

Aim: The aim of this study is to calculate neutron contamination at the presence of circular cones irradiating by 18 MV photons using Monte Carlo code.

Background: Small photon fields are one of the most useful methods in radiotherapy. One of the techniques for shaping small photon beams is applying circular cones made of lead. Using this method in high energy photon due to neutron contamination is a crucial issue.

Materials and methods: Initially, Varian linac producing 18 MV photons was simulated and after validating the code, various circular cones were also simulated. Then, the number of neutrons, neutron equivalent dose and absorbed dose per Gy of photon dose were calculated along the central axis.

Results: Number of neutrons per Gy of photon dose had their maximum value at depth of 2 cm and these values for 5, 10, 15, 20 and 30 mm circular cones were 9.02, 7.76, 7.61, 6.02 and 5.08 ($n\text{ cm}^{-2}\text{ Gy}^{-1}$), respectively. Neutron equivalent doses per Gy of photon dose had their maximum at the surface of the phantom and these values for mentioned collimators were 1.48, 1.33, 1.31, 1.12 and 1.08 (mSv Gy^{-1}), respectively. Neutron absorbed doses had their maximum at the surface of the phantom and these values for mentioned collimators sizes were 103.74, 99.71, 95.77, 81.46 and 78.20 ($\mu\text{Gy/Gy}$), respectively.

Conclusions: As the field size gets smaller, number of neutrons, equivalent and absorbed dose per Gy of photon increase. Also, neutron equivalent dose and absorbed dose are maximum at the surface of phantom and then these values will be decreased.

© 2018 Greater Poland Cancer Centre. Published by Elsevier Sp. z o.o. All rights reserved.

* Corresponding author at: Joint Cancer Research Center, Radiotherapy Oncology & Radiobiology Research Center, Cancer Institute, Tehran University of Medical Sciences, Tehran, Iran.

E-mail address: nedaieha@sina.tums.ac.ir (H.A. Nedaie).<https://doi.org/10.1016/j.rpor.2017.12.001>

1507-1367/© 2018 Greater Poland Cancer Centre. Published by Elsevier Sp. z o.o. All rights reserved.

1. Background

External Beam Radiation Therapy (EBRT) is the most popular form of radiotherapy. Linear accelerators (Linacs) that produce electrons or X-rays at energies of 4–25 MV are usually used for EBRT delivering. Linacs enable administration of high doses of X-rays to deep seated tumors. Also, these accelerators produce unintended radiation source like scattered radiation from the head of the accelerator and inside the patient body, leakage radiation from different parts of machines, and when the photon energy is high enough, secondary neutrons are produced from photonuclear interactions.^{1,2} These photoneutrons are produced in a range of energy associated with higher radiobiological damages and sometimes secondary malignancies are reported as the late effect of the produced photoneutron.³

Small photon fields are increasingly used in modern radiotherapy techniques, especially in Intensity Modulated Radiation Therapy (IMRT) and Stereotactic Radio-Surgery (SRS) treatments.³ Stereotactic means knowing the accurate site of the target. For this aim, the patient should be in a fixed three-dimensional coordinate system which is referenced to a point in the treatment room. SRS is performed by Gamma knife and linac in small photon fields.^{4–6}

One way to produce small photon fields in linac based SRS is using the circular cones that can be attached to a linac head as an accessory. Therefore, X-rays from the machine are collimated into fine beams and precisely focused on the target and small fields with sharp penumbras and steep dose gradients external to the treatment volume, are yielded.^{5,7,8}

By considering the crucial role of small field radiotherapy, it is important to be aware of different aspects of this technique in high energy photon beams. One of the most critical issues is neutron contamination.

The main photoneutron source in radiotherapy technique is the Giant Dipole Resonance (γ, n) reaction with high Z materials in the linac head. Since the cross section of photoneutron production in high Z materials is more than low Z materials (W: 400 mb; C: 8 mb), the linac head provides the major contribution in neutron contamination. The resulting neutrons can travel through a treatment room and a maze, thus not only the patients but also the staff are affected by neutrons. The probability of photoneutron interaction increases steeply with photon energy and the energy threshold of the (γ, n) reactions is about 8 MeV for most of isotopes. On the other hand, the absorption cross sections of materials in the accelerator head are not enough for shielding neutrons. Therefore, such neutrons will irradiate the patient and they contribute to an additional dose which is not taken into account in routine radiotherapy treatment. Due to high Z material (lead) in circular cones and their high cross section of photoneutron interactions, it is important to be aware of the circular cones effects on neutron generation irradiating by 18 MV photon beam in small photon fields.^{9–11} The dosimetry of neutrons in mixed photon-neutron fields has many difficulties that cause uncertainty of more than 10%. Therefore, Monte Carlo (MC) simulation seems to be a reliable solution because the dose contribution from each type of particle can be calculated separately.¹²

2. Aim

The aim of this study is to calculate neutron fluences, neutron equivalent dose and neutron absorbed dose per Gy of photon dose in the presence of various circular cones and 18 MV photon beams using MCNPX MC simulation.

3. Materials and methods

3.1. MC simulation

For calculating the neutrons contributions to the dose absorbed, MCNPX MC simulation was applied. To access this aim, initially, the detailed geometry of Varian Clinac 2100 C/D Linac head (including target (W,Cu), primary collimators (W), flatterer filter (Ta,Fe), ion chambers (Kapton) and collimator jaws (W)) were simulated according to the information of the manufacturer and previous studies.^{13,14} Also, a cubic water phantom with dimension of 30 cm \times 30 cm \times 40 cm at the distance of 100 cm from the source (SSD = 100 cm) was simulated.¹⁵

3.2. MC validation

For validating the simulation, the percentage depth dose (PDD) and beam profile of simulated geometry were compared with those of practical dosimetry. For this purpose, a point-like source emitting electrons in a single direction and a 0.2 cm radius disk, were chosen. Initial electrons had a Gaussian energy distribution with a Full Width at Half Maximum (FWHM) of 1 MeV and the peak energy of 18.37 MeV for photon beams. The jaws were fixed to produce a 10 cm \times 10 cm field size for SSD of 100 cm. Energy deposition was calculated by *F8 tally in 1.75 cm \times 1.75 cm \times 0.1 cm cells at the central axis to calculate the PDD. Calculation of beam profile was also performed by *F8 tally in 0.1 cm \times 1.75 cm \times 1.75 cm cells which were located at the vertical direction of the central axis at depth of 5 cm in the water phantom. Energy cut off for electrons and photons was 0.5 and 0.1 MeV, respectively. The code was run in photon-electron mode and also 2×10^9 particles were chosen for code running, the estimated statistical relative error of this simulation was about 2.3%. Then measurements of both depth dose and beam profile were performed by a Semiflex ionization chamber (PTW, Freiburg, Germany) at SSD of 100 cm and 10 cm \times 10 cm field size, similar to simulation situations.

The procedure of neutrons production and tracking of them was simulated by MCNPX version 2.6 and its library, this procedure was benchmarked for neutron fluence and energy spectra of neutrons in the study of Kry et al.^{16,17}

3.3. Neutron calculation

In this section, various circular cones made of lead producing field sizes of 5, 10, 15, 20 and 30 mm diameters were added to the simulation. The fourth entry on the PHYS:P card was set to -1 in order to activate photoneutron generation in code.¹² The cells used for this part were of size 2 cm \times 2 cm \times 0.5 cm.

The number of histories for neutron dose calculation was 2×10^9 and code was running in the electron-photon-neutron mode.

F4 tally was used to calculate the neutron fluence (ϕ) in terms of ($n \text{ cm}^{-2}/\text{electron}$) at the central axis as a function of depth.

Neutron equivalent dose (H) was measured by flux to equivalent dose conversion factors according to NCRP 38 Reports.¹⁸ The flux-to-dose equivalent conversion factors, which are energy dependent, were entered in the input files of MCNP by dose energy (DE) and dose function (DF) cards.¹⁹ Finally, H in terms of (mSv/electron) that defines the biological effects of neutrons was obtained as a function of depth.

Additionally, the absorbed dose from neutrons was measured by F6 tally in terms of ((MeV/g)/electron) that was converted to ((J/kg)/electron) for indicating the absorbed dose as a function of depth in terms of (Gy/electron). This tally does not include the contribution of capture gamma rays. Therefore, only energies transferred to recoil nucleus were afforded.

4. Results

Fig. 1 shows the geometry of linac and circular cone which were simulated for calculation of neutron quantities. Visual software (visedX22S) was applied for depicting this figure.

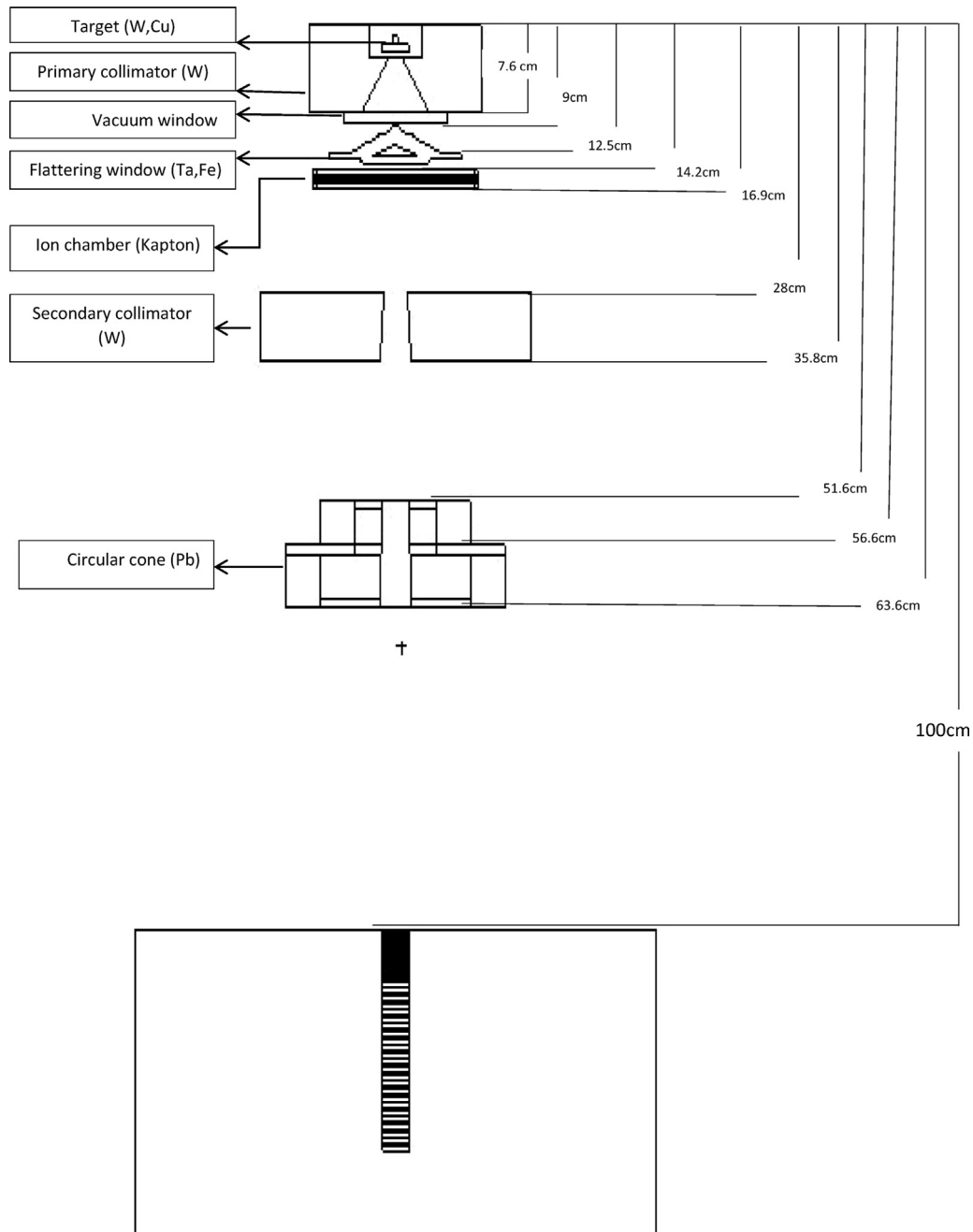


Fig. 1 – Schematic of Varian Clinac 2100 C/D linac head and circular cones obtained by simulation.

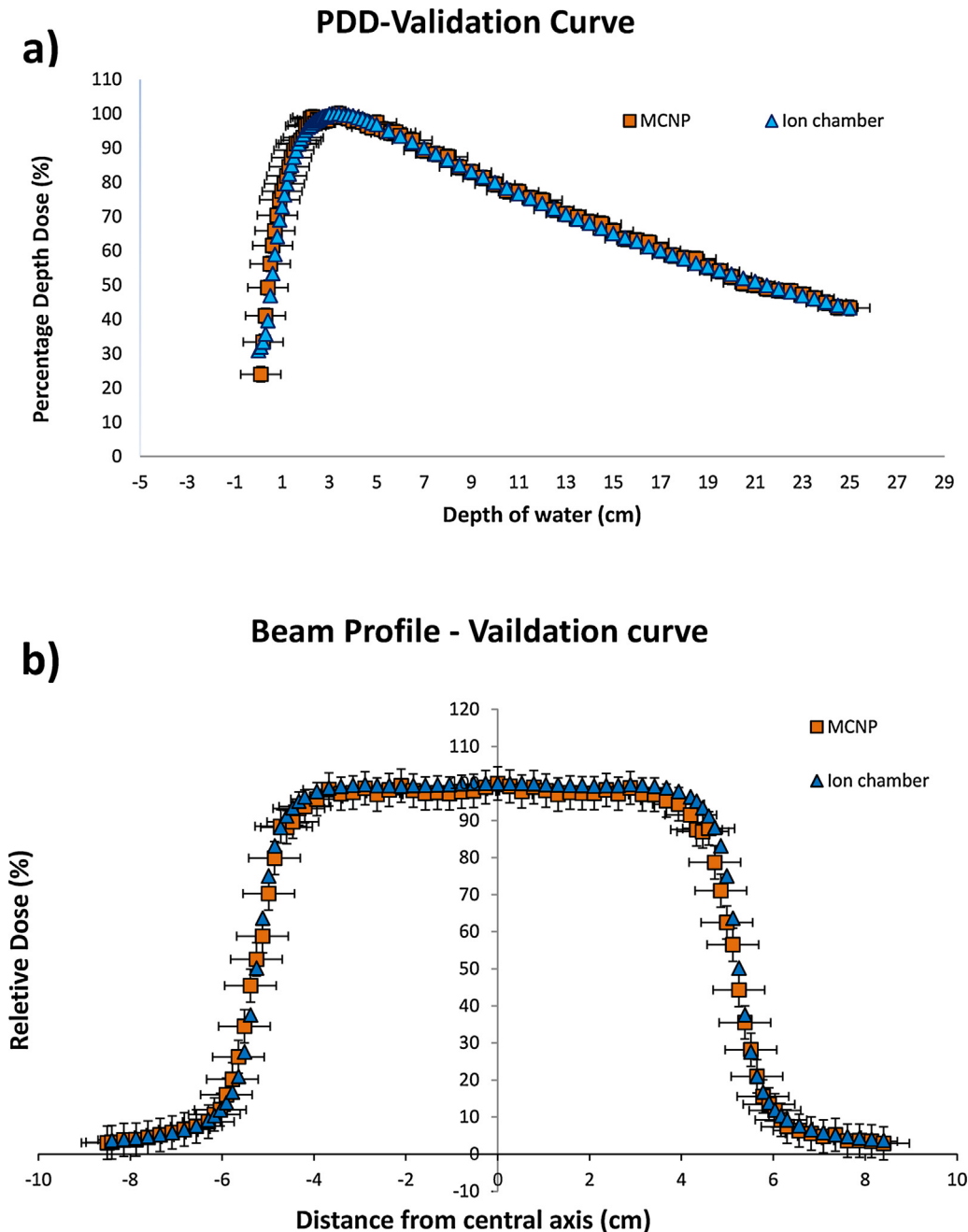


Fig. 2 – Comparison of MC results and ion chamber measurements as validation parameters: (a) Percentage depth dose 10 cm × 10 cm field size SSD of 100 cm. (b) Beam profile at depth of 5 cm, 10 cm × 10 cm field size and SSD = 100 cm.

Fig. 2(a and b) depicts the PDD and beam profile curves of the 10 cm × 10 cm field irradiated by 18MV photon beams, obtained by MCNPX code and semiflex ion chamber as the simulation validation parameters. As is indicated in Fig. 2, a general acceptable agreement is achieved between calculated and measured PDD and profile curves.

Table 1 indicates the comparison of the acquired data by simulation and ion chamber.^{13–20} Electrons are the starting particles in this study therefore all MCNP results are calculated in terms of per electron. Additionally, a normalization factor that makes the simulation data related to neutron quantities which are used in radiotherapy treatment has been

calculated.⁹ Fig. 3 indicates the depth dose in central axis per initial electrons for various circular cones. Finally, the neutron fluence, absorbed dose and neutron dose equivalent are calculated relative to the number of initial electrons needed to generate a photon absorbed dose of 1 Gy in the maximum dose depth (d_{max}).²¹ Table 2 shows the maximum values of photon absorbed dose in the presence of various circular cones.

In order to make the neutron fluence related to radiotherapy treatment situation, as explained in previous section, the output of F4 tally was normalized to the maximum photon dose at d_{max} and number of neutrons per Gy of photon in terms of ($n \text{ cm}^{-2} \text{ Gy}^{-1}$) was obtained in each depth of the phantom.

Table 1 – Comparison of PDD and beam profile obtained by MC simulation and ion chamber.

Parameter		Ion chamber	Monte Carlo	Difference
Percentage depth dose	Max difference at build up region (%)	–	–	0.93%
	R ₅₀ (cm)	0.4 cm	0.4 cm	0
	R ₈₀ (cm)	1.2 cm	1.1 cm	0.1
	R ₉₀ (cm)	1.6 cm	1.5 cm	0.1
	Max dose point (cm)	3.3 cm	3.2 cm	0.1
Beam profile	Max difference at flat region (%)	–	–	2.6%
	Max difference at penumbra region (%)	–	–	6%
	FWHM (cm)	10.5	10.37	0.13

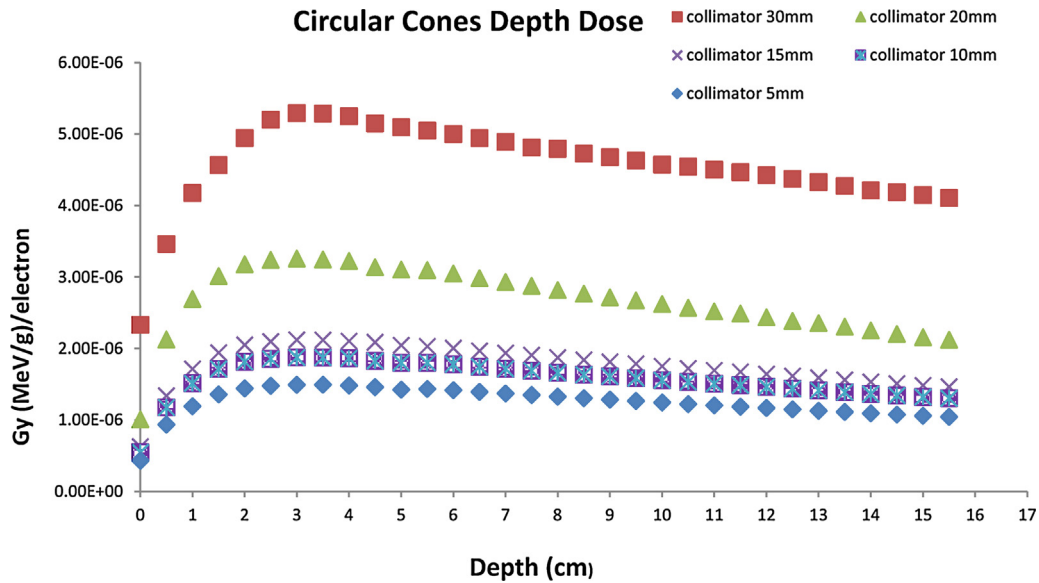


Fig. 3 – Depth doses of various circular cones.

Table 2 – Photon absorbed dose in d_{max} water phantom for different field size.

Diameters of different field sizes	Photon dose in d _{max} (Gy/electron)
30	8.47E–16
20	5.19E–16
15	3.39E–16
10	3.00E–16
5	2.39E–16

Fig. 4 shows the number of neutrons per Gy of photon dose as a function of depth in the presence of different circular cones. Table 3 shows the maximum values for the number of neutrons per Gy of photon dose in specific depth of phantom for different collimators.

Fig. 5 shows the neutron equivalent dose (H) values along the central axis as a function of depth in the presence of 5 different circular cones. Also, these values were normalized to the maximum photon dose at d_{max}. Since the maximum values for H are at the surface of the phantom, the comparison between these values for different field sizes at the surface of the phantom are shown in Table 4.

Neutron absorbed dose (D) was obtained by F6 tally that was in terms of ((MeV/g)/electron) and was converted to ((J/kg)/electron) which indicates absorbed dose as (Gy/electron). Also, the results are reported in terms of μGy/Gy

to define absorbed dose relative to the photon dose at maximum depth with different cones. Fig. 6 indicates neutron absorbed dose relative to photon dose in different circular cones as a function of depth. Since the maximum values for D occurred at the surface of the phantom, the comparisons between these values for different field sizes at the surface of phantom are shown in Table 5.

5. Discussion

As is shown in Fig. 4, the number of neutrons per Gy of photon increases at the first depth of the phantom until it reaches a maximum value at depth of 2cm and then decreases. In fact, neutrons in the first depths of phantom have higher energies. These neutrons have interactions with water. Therefore, they lose energy until they become thermal. As the number of fast neutrons decreases, the number of thermal neutrons increases and this increase is more than the reduction of fast neutrons. Therefore, their number increases until it reaches a maximum value. At this point, via the ¹⁴N(n,p)¹⁴C and ¹H(n,γ)²H reactions, the number of neutrons is reduced monotonically.²¹

As the field size gets smaller, the number of neutrons per Gy of photon dose increases. In smaller field sizes, the photon-neutron interactions increase, because the amount of

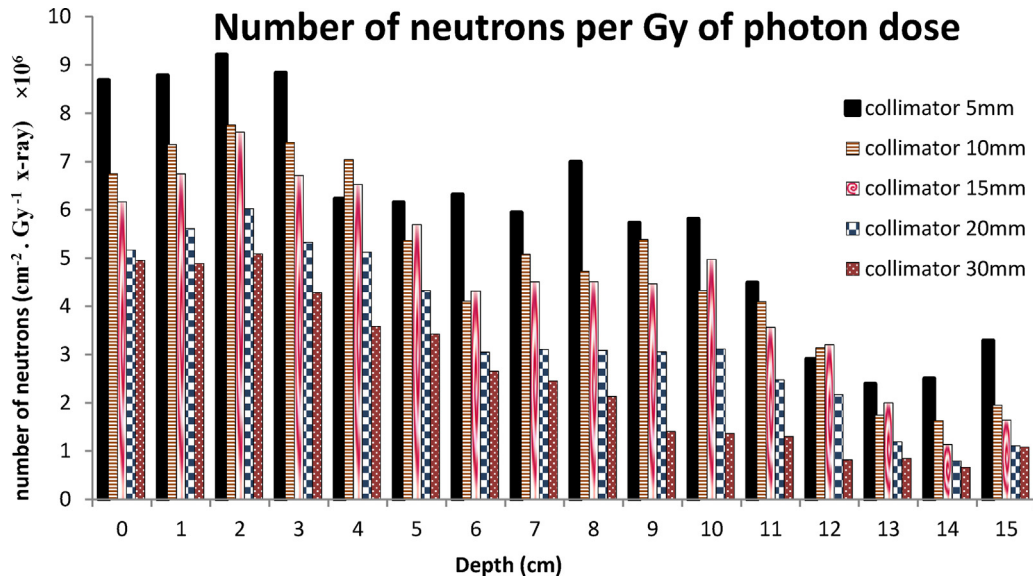


Fig. 4 – Number of neutrons per Gy of photon dose as a function of depth for different circular cones.

Table 3 – Maximum number of neutrons and depth of maximum values producing by presence of various circular cones.

Diameter of field (mm)	Max number of neutron per photon dose [$n \text{ cm}^{-2} \text{ Gy}^{-1}$]	d_{max} (cm)
30	5.08×10^6	2
20	6.02×10^6	2
15	7.61×10^6	2
10	7.76×10^6	2
5	9.20×10^6	2

Table 4 – Maximum values of neutron equivalent doses at the surface of the phantom producing by presence of various circular cones.

Neutron equivalent dose per photon dose (mSv/Gy)	Diameter of field (mm)
1.08	30
1.12	20
1.33	15
1.31	10
1.48	5

high Z materials, present in the way of high energy photons increased. Hence, the number of neutrons generation due to the presence of circular cones is increased.^{19,22,23}

The neutron equivalent dose has its maximum at the initial depths of the phantom and then decreases monotonically. Since neutrons in the first depths of the phantom have higher

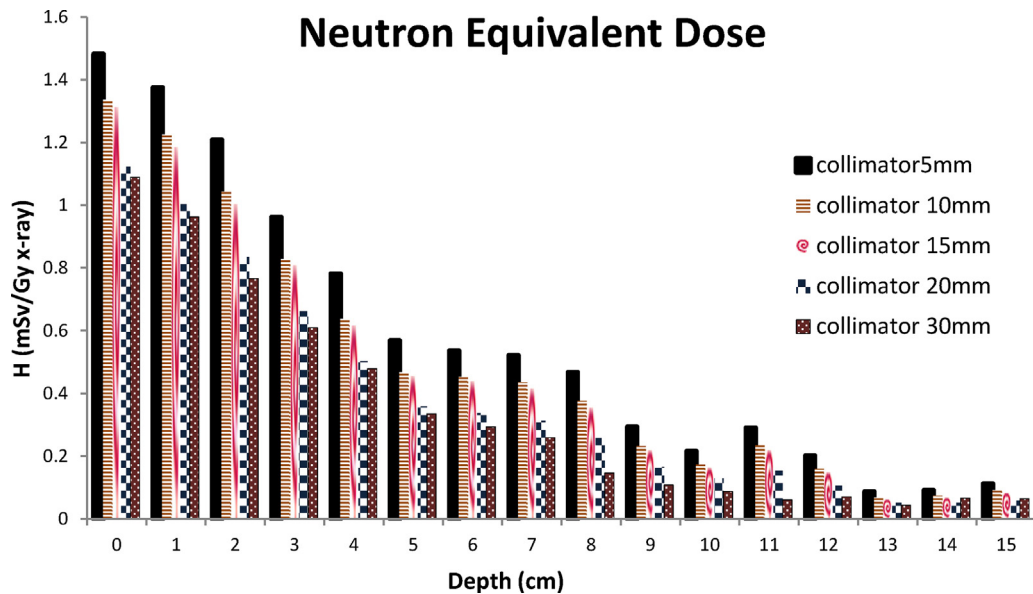


Fig. 5 – Neutron equivalent dose as a function of depth in water phantom for different field sizes.

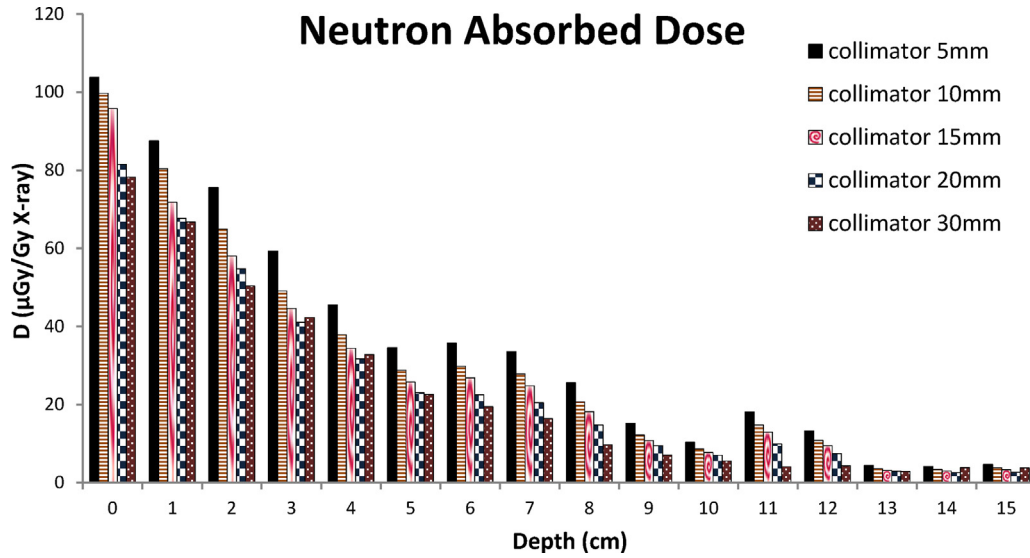


Fig. 6 – Neutron absorbed dose relative to photon dose as a function of depth for different field sizes.

Table 5 – Maximum neutron absorbed dose at the surface of the phantom producing by presence of various circular cones.

Neutron absorbed dose per photon dose (µGy/Gy)	Diameter of field (mm)
78.20	30
81.46	20
95.77	15
99.71	10
103.78	5

energies, the quality factors for these fast neutrons are more than thermalized neutrons. Consequently, in deeper cells as the neutron thermalizes, H will be reduced. Therefore, it is clear that appropriate attention to the depth of organs of interest is essential in estimating the neutron equivalent dose.²² On the other hand, regarding Fig. 5 and Table 3, the highest amount of neutron equivalent dose is associated with the presence of 5 mm circular cone and is 1.48 (mSv Gy⁻¹). As the field size became smaller, the neutron equivalent dose increased, because the cross-section of photoneutron interaction in high Z material of cones (lead) increased at smaller fields.

As shown in Fig. 6, the absorbed dose decreases with increasing depth. Since the neutron energy decreases in deeper cells, (D) will decrease. By considering the increases of photoneutron interaction in smaller field, it is acceptable that the absorbed dose in smaller fields, is higher than larger ones.

6. Conclusions

The results of this study indicates that all of neutron characteristic quantities, including the number of neutrons, neutron equivalent dose and absorbed dose per Gy of photon dose had their maximum values in the presence of 5 mm circular cones, because in this field photoneutron interaction

increased. Reduction of neutron equivalent dose in deeper cells indicates that organs at initial depths will be affected more than deeper ones by neutron contamination.

Conflict of interest

None declared.

Financial disclosure

None declared.

REFERENCES

- Xu XG, Bednarz B, Paganetti H. A review of dosimetry studies on external-beam radiation treatment with respect to second cancer induction. *Phys Med Biol* 2008;53:R193–241.
- Murray LJ, Robinson MH. Radiotherapy: technical aspects. *Medicine* 2015;44(1):10–4.
- Ghiasi H. Monte Carlo characterizations mapping of the (γ, n) and (n, γ) photoneuclear reactions in the high energy X-ray radiation therapy. *Rep Pract Oncol Radiother* 2014;19:30–6.
- Yarahmadi M, Nedaie HA, Allahverdi M, Asnaashari KH, Sauer OA. Small photon field dosimetry using EBT2 Gafchromic film and Monte Carlo simulation. *Int J Radiat Res* 2013;11(4):215–24.
- Chin LS, Regine WF. *Principle and practice of stereotactic radiosurgery*. New York, NY: Springer; 2007.
- Nabavi M, Nedaie HA, Salehi N, Naderi M. Stereotactic radiosurgery/radiotherapy: a historical review. *Iran J Med Phys* 2014;11(1):156–67.
- Esnaashari KN, Allahverdi M, Gharaati H, Shahriari M. Comparison of measured and Monte Carlo calculated dose distributions from circular collimators for radiosurgical beams. *Iran J Radiat Res* 2007;5(1):31–6.
- Sharma SD, Kumar S, Dagaonkar SS, et al. Dosimetric comparison of linear accelerator-based stereotactic radiosurgery systems. *Med Phys* 2007;32(1):18–23.

9. Zanini A, Durisi E, Fasolo F, et al. Monte Carlo simulation of the photoneutron field in linac radiotherapy treatments with different collimation systems. *Phys Med Biol* 2004;**49**:571–82.
10. Pena J, Franco L, Gómez F, Iglesias A, Pardo J, Pombar M. Monte Carlo study of Siemens PRIMUS photoneutron production. *Phys Med Biol* 2005;**50**:5921–33.
11. Konefal A, Orlef A, Laciak M, Ciba A, Szewczuk M. Thermal and resonance neutron generated by various electron and X-ray therapeutic beams from medical linacs installed in polish oncological centers. *Rep Pract Oncol Radiother* 2012;**17**:339–46.
12. Chibani O, Ma CM. Photonuclear dose calculations for high-energy photon beams from Siemens and Varian linacs. *Med Phys* 2003;**30**(8):1990–2000.
13. Alem-Bezoubiri A, Bezoubiri F, Badreddine A, Mazrou H, Lounis-Mokrani Z. Monte Carlo estimation of photoneutrons spectra and dose equivalent around an 18 MV medical linear accelerator. *Radiat Phys Chem* 2014;**97**:381–92.
14. Sheikh-Bagheri D. *Monte Carlo methods for accelerator simulation and photon beam modeling*. Windsor, Allegheny General Hospital Pittsburgh, PA: AAPM Summer School; 2006.
15. Version MUM 2.6.0, April 2008, LA-CP 07-1473.
16. Kry SF, Howell RM, Salehpour M, Followill DS. Neutron spectra and dose equivalents calculated in tissue for high-energy radiation therapy. *Med Phys* 2009;**36**(4):1244–50.
17. Kry SF, Titt U, Followill D, et al. A Monte Carlo model for out-of-field dose calculations from high-energy photon therapy. *Med Phys* 2007;**34**:3489–99.
18. NCRP 38. *Protection against neutron radiation*. National Council on Radiation and Protection and Measurement; 1971.
19. Mohammadi N, Miri-Hakimabad H, Rafat-Motavalli AF, Abdollahi S. Neutron spectrometry and determination of neutron contamination around the 15 MV Siemens Primus LINAC. *J Radioanal Nucl Chem* 2015;**304**:1001–8.
20. Venselaar J, Welleweerd H, Mijnheer B. Tolerances for the accuracy of photon beam dose calculations of treatment planning systems. *Radiother Oncol* 2001;**60**:191–201.
21. Ovalle M, Barquero SA, Gomez-Ros JM, Lallena AM. Neutron dose equivalent and neutron spectra in tissue for clinical linacs operating at 15, 18 and 20 MV. *Radiat Protect Dosim* 2011;**147**(4):498–511.
22. Naseri A, Mesbahia A. A review on photoneutrons characteristics in radiation therapy with high-energy photon beams. *Rep Pract Oncol Radiother* 2010;**15**:138–44.
23. Ma A, Awotwi-Pratt J, Alghamdi A, Alfuraih A, Spyrou NM. Monte Carlo study of photoneutron production in the Varian Clinac 2100C linac. *J Radioanal Nucl Chem* 2008;**276**(1):119–23.